*Desalination and Water Treatment*
www.deswater.com
doi: 10.1080/19443994.2014.1000383

57 (2016) 4255–4266
February

Taylor & Francis
Taylor & Francis Group

# Development of nano-crosslinked polyacrylonitrile ions exchanger particles for dyes removal

M.S. Mohy Eldin[a,*], Y.A. Aggour[b], M.R. El-Aassar[a], G.E. Beghet[b], R.R. Atta[b]

[a]*Polymer Materials Research Department, Advanced Technology and New Materials Research Institute, MuCSAT, New Boarg El-Arab City, Alexandria 21934, Egypt, Tel. +203 4593 414; emails: m.mohyeldin@mucsat.sci.eg (M.S. Mohy Eldin), mohamed_elaassar@yahoo.com (M.R. El-Aassar)*
[b]*Faculty of Science at (New) Damietta, Physical Chemistry, Department of Chemistry, Damietta University, Damietta, Egypt, Tel. +2057 2403866; emails: yassina9@yahoo.com (Y.A. Aggour), GamalBekheit@du.edu.eg (G.E. Beghet), ramadanatta75@du.edu.eg (R.R. Atta)*

Received 18 April 2014; Accepted 16 November 2014

ABSTRACT

Poly(acrylonitrile-co-divinylbenzene) nanoparticles, approximately 41 nm mean size, were prepared by precipitation polymerization technique in water:ethanol phase. Influence of the various polymerization parameters (e.g. temperature and time of polymerization, concentration of monomers and initiator, monomers composition, and cosolvent ratio) on the properties (e.g. size and conversion yield) of the particles have been investigated. Poly (acrylonitrile-co-divinylbenzene) nanoparticles were functionalized with amidoxime groups through chemical modification using hydroxyl amine to acquire ions exchanger characters. As a result, the particle size of the copolymer was increased from 41 up to 46 nm. The verification of the hydroximation process was obtained from thermogravimetric and infrared spectrometer analyses. The influence of various parameters, such as the concentration of hydroxyle amine, the temperature and the time of amidooximation, and the monomers composition, on the ion exchange capacity has been investigated and correlated finally to the efficiency of methylene blue removal process.

*Keywords:* Poly (acrylonitrile-co-divinylbenzene) nanoparticles; Precipitation polymerization; Dye removal; Adsorption; Methylene blue; Amidoxime-modified polyacrylonitrile

## 1. Introduction

During the past three decades, several physical, chemical, and biological decolorization methods have been reported; few, however, have been accepted by the paper and textile industries. Amongst the numerous techniques of dye removal, adsorption using different adsorbents is the procedure of choice and gives the best results as it can be used to remove different types of coloring materials [1–3].

PAN fibers are known for their dye ability toward cationic (basic) dyes [4–6]. Rosenbaum studied dyeing of PAN with cationic dye (Malachite Green) [4,5] and monitoring the diffusion rates and models. Hossain et al. [6] reviewed the diffusion of cationic dyes into PAN. Recently, Şuteu et al. [7] presents new results about efficiency of wastes based on hydrolyzed Poly Acrylonitrile textile fibers (HPAN) as sorbents in

*Corresponding author.

1944-3994/1944-3986 © 2015 Balaban Desalination Publications. All rights reserved.

removal of some dyes from textile effluents. The effect of some experimental variables such as initial dye concentration, sorbent mass, pH, temperature, and contact time were investigated. The sorbent–dye sorption systems are described using Freundlich, Langmuir, and Dubinin–Radushkevich isotherm models. The laboratory experimental results performed using the textile fibers' wastes indicate the good removal of dyes from aqueous medium, suggesting that these textile solid wastes correspond to the actual tendency of using nonconventional sorbtive materials to reduce the overall cost of sorbent preparation. The surface area of the adsorbent materials is a determined factor. Nanoadsorbents with high surface area are the optimum choice to have efficient adsorption process.

PAN nanoparticles have been prepared using different techniques [8–11]. Boguslavsky et al. [8] prepared PAN nanoparticles in sizes ranging from approximately 35–270 nm by dispersion/emulsion polymerization of acrylonitrile in a continuous aqueous phase in the presence of potassium persulfate (KPS) as initiator and various alkyl-sulfate and sulfonate surfactants. Biswal et al. [9] synthesised PAN nanoparticles under the catalytic effect of in situ-developed Co (II)/EDTA complex with ammonium persulphate as initiator, in the absence of emulsifier. Later on, the same authors developed the process under simple microwave conditions [11]. Lee et al. [10] prepared poly(acrylonitrile-co-itaconicacid-comethylacrylate) nanoparticles by aqueous dispersion polymerization using hydrophilic PVA in a water/N, N-dimethylformamide mixture media.

In the present study, first, Poly(acrylonitrile-co-divinylbenzene) nanoparticles were prepared by precipitation polymerization technique in water:ethanol (ETOH) phase and then, the nitrile groups were chemically modified to amidoxime ones in the second step. Finally, the oxime-functionalized nanoparticles were applied for removal of MB from the MB dye aqueous solution.

## 2. Materials and methods

### 2.1. Materials

The following analytical grade chemicals were purchased from commercial sources and were used without further purification: acrylonitrile (AN) (Aldrich, 99%), divinyl benzene (DVB) (Aldrich, technical grade, 80%), KPS extra pure (Loba Chemie, 98%), ETOH absolute (Aldrich, 99.9%), hydroxylamine hydrochloride (HA) (Adwic, 97%), sodium hydroxide (NaOH) (99%), sodium chloride (NaCl) (99%), and methylene blue (MB) (Alpha Chemika, 82%). Distilled water was employed in all reactions.

### 2.2. Scanning electron microscopic analysis

The scanning electron microscope (SEM) images of the copolymer particles were obtained by placing the particles onto carbon tape-attached aluminum SEM stubs after coating with gold to a few nanometer thicknesses under vacuum.

### 2.3. Fourier transform infrared spectroscopic analysis

The Fourier transform infrared spectroscopic (FTIR) spectra of the copolymer particles were recorded with a FTIR spectrometer in the spectral range 4,000–500 $cm^{-1}$.

### 2.4. Thermogravimetric analysis

The thermal analysis of the copolymer particles was carried out using a thermogravimetric analyzer (TGA). About 6 mg of particles were placed in ceramic pans of TGA instrument and analyzed over the temperature range 0–600°C with the heating rate of 10°C/min under dry $N_2$ flow at the rate of 10 mL/min.

### 2.5. Particles size analysis

The particles size distribution was monitored using submicron particle size analyzer (PSA) though dispersed the copolymer samples in ETOH.

### 2.6. Preparation of the copolymer nanoparticles

In a test tube, predetermined weight of KPS was dissolved first in water and then equal ETOH volume was added to have 0.01 M final KPS concentration. Selected equal volumes from monomers DVB and AN were then added to have 10% final co-monomers concentration. The mixture was stirred well to have a homogenous solution. The polymerization vessel was then thermoincubated at predetermined temperature (55°C) and the polymerization reaction was conducted for 4 h. After completion the polymerization time, the copolymer was collected and successively washed with (Water/ETOH) solution to remove unreacted monomers. Centrifugation at 8,000 rpm for 30 min using ultra speed centrifuge was used to separate the copolymers particles. The copolymer was then dried at 80°C for 24 h before weighted. The efficiency of the copolymerization process was evaluated by calculating

the percentage of monomers converted to copolymer according to the following formula:

$$\text{Conversion yield } (\%) = [W_1/W_0] \times 100 \quad (1)$$

where $W_0$ is the weight of the monomers and $W_1$ is the weight of the copolymer.

### 2.7. Poly(acrylonitrile-co-divinylbenzene) amidoximation

To have amidoxime functionalized poly(acrylonitrile-co-divinylbenzene) (P(AN-co-DVB)), 1 g of the copolymer was reacted with 50 mL of 1% HA at 60°C for 4 h. After completion of the functionalization reaction time, the hydroximated poly(acrylonitrile-co-divinylbenzene) (HP(AN-co-DVB)) particles were centrifuged at 8,000 rpm for 30 min to remove unreacted HA, then treated with 30 mL of 2% NaOH solution at room temperature for 1 h. The modified copolymer particles were then successively washed with distilled water to remove excess of NaOH and finally dried at 80°C for 24 h. The dried copolymer particles were then used in the ion exchange capacity (IEC) measurements and the MB adsorption experiments.

### 2.8. Ion exchange capacity

The IEC of HP (AN-co-DVB) copolymer nanoparticles was determined using acid–base titration. Weighed sample (0.1 g) was immersed in 2 M NaCl solution (20 mL) at room temperature (R.T) for 24 h. The solution was then titrated with 0.001 M NaOH solution. IEC was calculated as follows:

$$\text{IEC}(\text{meq}-1) = \frac{n(\text{mmol})}{(\text{cm}^3)} \times \frac{v(\text{cm}^3)}{w(\text{g})} \quad (2)$$

where $n$, $v$, and $w$ are the concentration of the NaOH solution, the volume of the NaOH solution, and the weight of the sample, respectively [12].

### 2.9. Preparation of basic dye solution

MB, $C_{16}H_{18}N_3SCl_3H_2O$, stock solution was prepared by dissolving 0.01 g of MB in 1,000 mL distilled water. The dye concentration in the supernatant and residual solutions was determined by measuring their absorbance in 1 cm light-path cell at Max wave length 660 nm using spectrophotometer.

### 2.10. Batch MB adsorption experiments

The adsorption experiments were carried out in a batch process using MB aqueous solution. The variable parameters namely, the initial MB concentration, the adsorbent amount, the contact time, and the adsorption temperature were studied. The MB adsorption studies were performed by mixing 0.1 g of HP (AN-co-DVB) with 50 mL of 10 ppm MB. The mixture was agitated at R.T in a shaking water bath for 4 h and then centrifuged at 8,000 rpm for 30 min to separate the adsorbent out of the liquid phase. The dye concentration, before and after the adsorption, for each solution was determined by measuring the absorbance at maximum wavelength ($\lambda_{max} = 660$ nm) using UV–vis spectrophotometer. Dye removal percentage was calculated according to the following formula:

$$\text{Dye removal } (\%) = [(C_0 - C_t)/C_0] \times 100 \quad (3)$$

where $C_0$ and $C_t$ (mg $L^{-1}$), are the initial concentration at zero time and the final concentration of MB at definite time, respectively.

## 3. Results and discussion

### 3.1. Preparation of the copolymer nanoparticles

Factors affecting the preparation step and its impact on both the conversion yield and the mean particle size are discussed in the following.

#### 3.1.1. Effect of the co-monomers concentration

Fig. 1 shows the effect of variation of the monomers concentration on the polymerization conversion

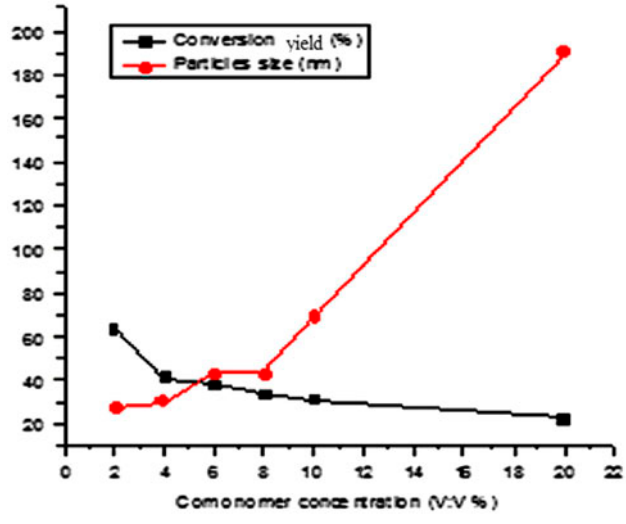


Fig. 1. Effect of the monomers concentration on the polymerization conversion yield and the particles size of P (AN-co-DVB).

yield and the particles size of the monomers and the copolymer, respectively. It is clear that increasing the comonomer concentration decreased the polymerization conversion yield and increased the particles size. The limitation of the initiator concentration and the availability of the monomers units may be explained the obtained behavior. In addition, the hydrophobicity of both monomers may be contributed in limiting of their solubility at high concentration which leads to decrease of the polymerization conversion yield and increase the particle size.

### 3.1.2. Effect of the comonomers composition

Fig. 2 shows the effect of variation of the comonomers composition on the polymerization conversion yield and the particles size of the copolymer. Inspection of the figure shows two observations. The first one indicated a gradual and constant decrease of the polymerization conversion yield with increasing the DVB content in the feeding comonomers solution. The second one indicated a decrease of the formed copolymer particles size, in which two stages have been observed. The first stage is fast, constant, and located at AN composition ranged from 100 to 40%. The second stage has less rate of particle size decrease located at AN composition ranged from 30 to 0%. To understand the obtained behavior, both monomers have been individually polymerized under the same conditions and the polymerization conversion yield was determined. From the obtained data it is obvious that the polymerization conversion yields of AN and DVB are 57 and 11%, respectively. The super reactivity of AN over DVB explained the obtained polymerization conversion yield and the particles size behavior.

### 3.1.3. Effect of the polymerization time

Fig. 3 reveals a similar behavior for both the polymerization conversion yield and the particles size at the first 4 hours stage of the polymerization reaction. After that, the polymerization conversion yield continues to increase with moderate rate from 35 to 52% during 4 h. On the other hand, the particles size was exponentially increased from 50 to 100 nm during 2 h, from 4 to 6 h, of the polymerization time. The reduction of the polymerization reaction rate after 4 h of polymerization time may be referred to consumption of the initiator radicals in the early stage of the polymerization step, which consequently leads to increase in the size of the formed copolymers particles.

### 3.1.4. Effect of the initiator concentration

Fig. 4 showed the effect of variation of the $K_2S_2O_8$ concentration on the polymerization conversion yield and the particles size. Linear increase of the polymerization conversion yield has been observed with increase in the $K_2S_2O_8$ concentration up to 0.02 M. Slight increase of the polymerization conversion yield was found with further increase of the $K_2S_2O_8$ concentration to 0.05 M. The increment of the polymerization conversion yield using $K_2S_2O_8$ concentration up to 0.02 M could be interpreted in terms of participation of the primary produced free radical species mainly in the initiation step of the copolymerization process

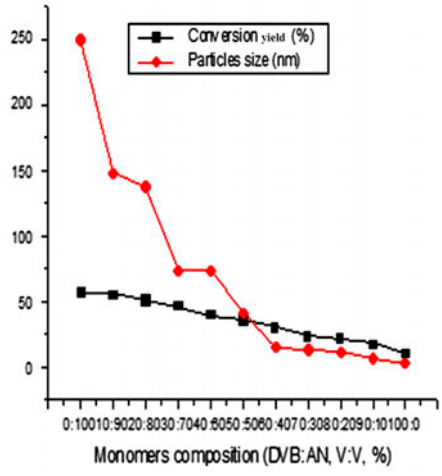


Fig. 2. Effect of the monomers composition on the polymerization conversion yield and the particles size of P (AN-co-DVB).

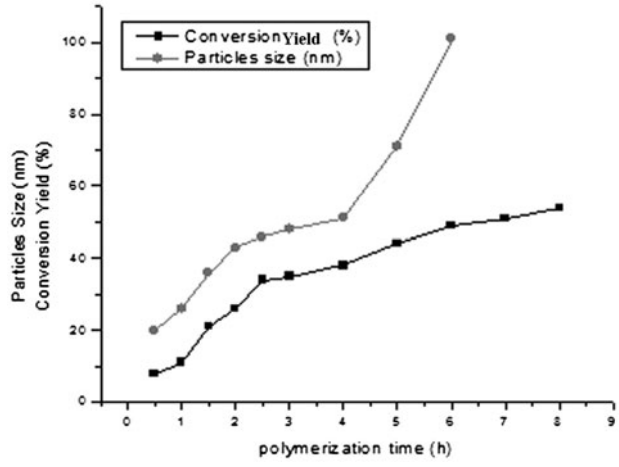


Fig. 3. Effect of the polymerization time on the polymerization conversion yield and the particles size of P(AN-co-DVB).

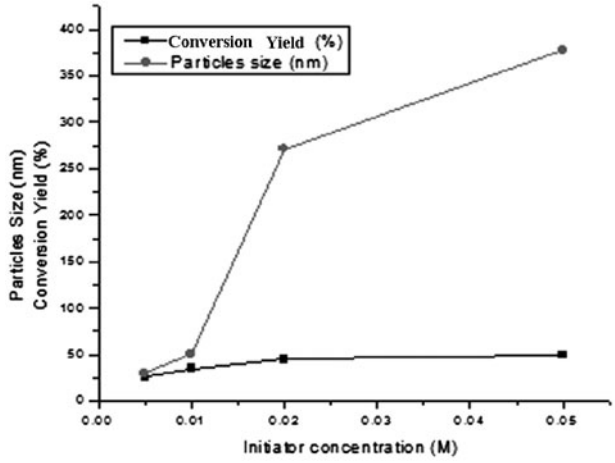


Fig. 4. Effect of the initiator concentration ($K_2S_2O_8$) on the polymerization conversion yield and the particles size of P (AN-co-DVB).

rather than the termination step. Using higher $K_2S_2O_8$ concentration leads to a balance between its contributions in both steps of the polymerization process [13]. On the other hand, the particles size showed different behaviors, where sudden increment of its value has been observed using higher initiator concentration than 0.01 M. The particles size has increased up to 275 and 380 nm using 0.02 and 0.05 M $K_2S_2O_8$, respectively.

A similar influence of the initiator concentration on the particles size has been previously reported by Tseng et al. [14], Shen et al. [15], and others [16–21]. According to their explanation, increasing the initiator concentration causes an increase in the oligomeric radicals' concentration, and thus in the number of P(AN-co-DVB) chains. This may lead to an increase in the number of P(AN-co-DVB) nanoparticles (more nuclei) and an increase in their size (more P(AN-co-DVB) chains participating in the growing process. Moreover, a higher initiator concentration increases the growth rate of the oligomeric chains, thus favoring secondary nucleation during the particle growth stage. On the other hand, the opposite effect, of decreasing the particle diameter by increasing the initiator concentration, was reported by Horák [22] in the dispersion polymerization of 2-hydroxyethyl methacrylate and by Capek [23–25], Sajjadi and Brooks [26] in emulsion polymerization of butyl acrylate and of methyl methacrylate with ethyl acrylate.

### 3.1.5. Effect of the cosolvent ratio ($H_2O$:ETOH)

The effect of variation of the cosolvent ratio ($H_2O$:ETOH) on the polymerization conversion yield and the particles size have been studied (Fig. 5). It is clear that increase in the water ratio in the polymerization medium has a negative effect on both parameters. This is may be attributed to the solubility limitation for both monomers, especially DVB in water. Accordingly, the polymerization conversion yield was reduced. On the other hand, the nonsolvent effect of water on the formed polymers' nuclei accelerates their precipitation in early formation stage with small particle size.

### 3.1.6. Effect of the polymerization temperature

As shown in Fig. 6, it is clear that the polymerization conversion yield was increased with increase in the polymerization temperature. Increasing of the reaction temperature accelerates the rate of initiator decomposition to give free radicals. This is expected since the rates of reactions are exponentially temperature-dependent functions according to Arrhenius law. On the other hand, rising the temperature increases the number of collisions between initiators and monomers molecules that lowers the reaction energy gap and promotes the polymerization process. Also, Fig. 6 illustrates the effect of the polymerization temperature on the formed particles size. Similar results indicating an increase in the polymeric particles diameter with increasing the polymerization temperature were reported for dispersion polymerization of styrene [27,28] methyl methacrylate [15], hydroxyethyl methacrylate [29], and of styrene with buthyl acrylate [30].

A possible explanation is increasing the polymerization temperature increases the $K_2S_2O_8$ decomposition rate (obtaining more radicals). Therefore, increasing the temperature is equivalent to increase of

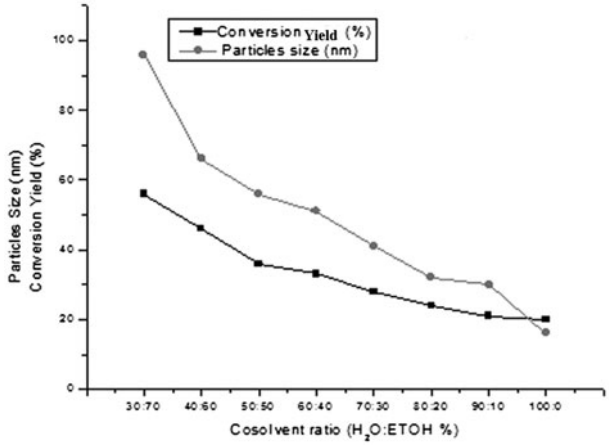


Fig. 5. Effect of cosolvent ratio ($H_2O$:ETOH) on the polymerization conversion yield and the particles size of P (AN-co-DVB).

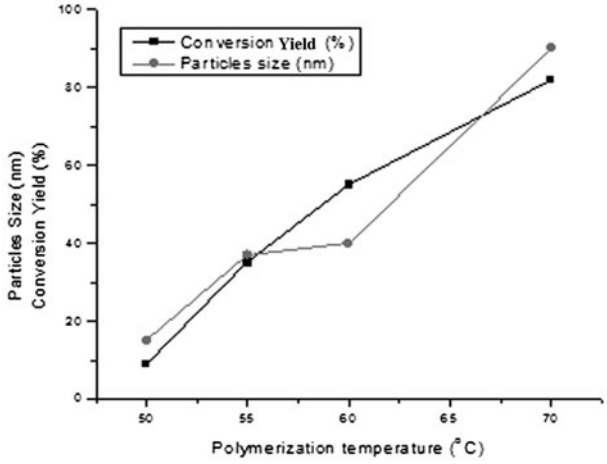


Fig. 6. Effect of the temperature on the polymerization conversion yield and the particles size of P(AN-co-DVB).

the initiator concentration, which leads to increase of the polymerization rate and subsequently of the particles size. However, contrary to increasing of the initiator concentration, increasing the polymerization temperature leads to an increase in the oligoradical reactivity and a decrease in their half-life period, thus achieving a faster particles growth rate and a more rapid attainment of their maximal size. According to Shen et al. [15,31], an increase in the polymerization temperature in dispersion polymerization systems leads, among other things, to the following effects: (1) an increase in the critical chain length of the oligoradicals due to the increase in the solvency of the continuous phase; (2) an increase in the concentration of precipitated oligomer chains (due to increase in both the decomposition rate of the initiator and the propagation rate of oligomer radicals). All of these effects may contribute to an increase in the particles size.

### 3.2. Characterization of poly(acrylonitrile-co-divinylbenzene) nanoparticles

#### 3.2.1. FTIR analysis

Fig. 7 presents the FTIR spectra of polymers PDVB, PAN, and P(AN-co-DVB). PAN is characteristic of the adsorption peaks at 2,248 $cm^{-1}$, which correspond to the bonds (C≡N). PDVB is characteristic of the adsorption peaks at 1,608 and 3,025 $cm^{-1}$, which correspond to the bonds of benzene ring and (=C–H), respectively. By comparing the FTIR spectrum of the copolymer with the spectrums of individual polymers, it can be seen that the P(AN-co-DVB) kept the absorptions at 2,248 $cm^{-1}$ for (C≡N) and 1,606 $cm^{-1}$ for benzene ring,

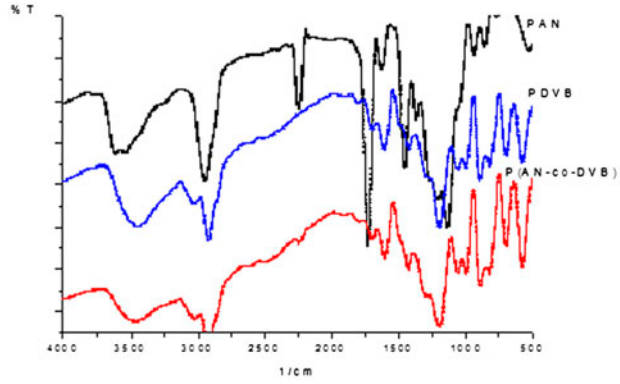


Fig. 7. FTIR spectra for PDVB, PAN, and P(AN-co-DVB).

indicating that the copolymer maintains the main characteristics of the individual monomers.

#### 3.2.2. TGA analysis

The curves in Fig. 8 showed the thermal decomposition of PDVB, PAN, and P(AN-co-DVB). It is obvious from the figure that the copolymer has acquired higher thermal stability than both individual polymers. This presents proof for the copolymer formation.

#### 3.2.3. SEM morphology

Fig. 9 shows SEM images of PDVB, PAN, and P (DVB-co-AN). From the figure, it is clear that the

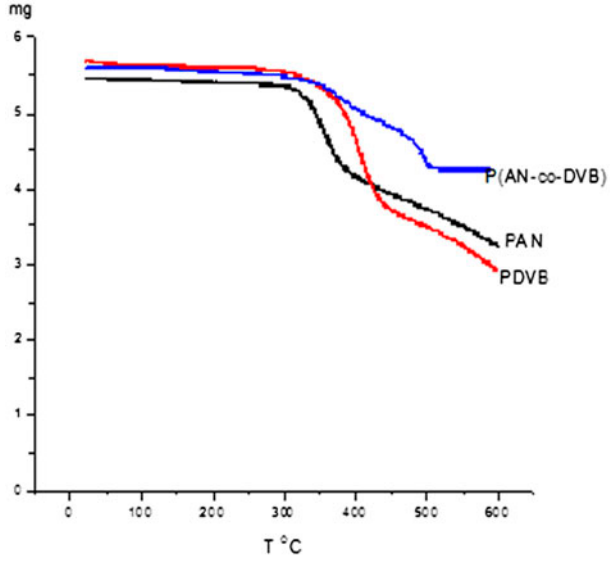


Fig. 8. TGA curve for PDVB, PAN, and P(AN-co-DVB).

changes in the surface morphology of P(DVB-co-AN) nanoparticles and formation of spherical particles with uniform distribution relative to the irregular forms of both PAN and PDVB.

### 3.3. Functionalization of poly(acrylonitrile-co-divinyl benzene)

Poly(acrylonitrile-co-divinylbenzene) nanoparticles were functionalized with amidoxime groups through chemical modification using hydroxyl amine to acquire ions exchanger characters. The effect of variation of the copolymer composition and the variation of the functionalization process conditions on the IEC has been investigated and a correlation between the IEC and the MB removal capacities of functionalized copolymer nanoparticles has been established.

#### 3.3.1. Effect of copolymers composition

The copolymer nanoparticles with different compositions prepared earlier (Fig. 1) have been functionalized under fixed conditions. Fig. 10 illustrates the correlation between the composition and IEC of HP (AN-co-DVB) copolymers. From the figure, it is clear that the IEC decreased from 0.070 to 0.025 (meq/g) with decrease in the poly AN content of the copolymer nanoparticles. This behavior is explained by the formation of less oximic exchangeable sites on the expense of P(AN-co-DVB)′ Nitrile groups.

On the other hand, Fig. 10 correlates the IEC of HP (AN-co-DVB) to its MB removal percentage. From the figure, it is clear that the MB removal percentage decreased with decrease the IEC. This behavior is explained by the progressive decrease of oximic exchangeable sites on the P(AN-co-DVB) surface and pores′ interiors [32].

#### 3.3.2. Effect of the amidoximation temperature

The effect of variation of the amidoximation temperature on the IEC of HP(AN-co-DVB) and its MB removal percentage was investigated (Fig. 11). From the figure, it is clear that the IEC and the MB removal percentage were increased with increase in the amidoximation temperature. This is expected since the rate of reaction is exponentially temperature-dependent function according to Arrhenius law.

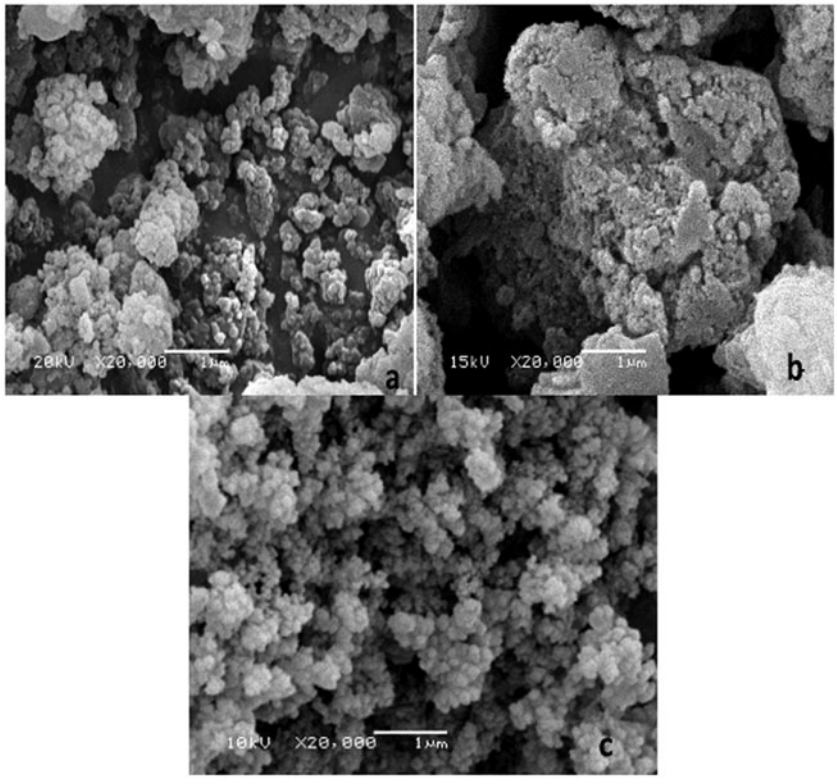


Fig. 9. SEM photographs of (a) PDVB, (b) PAN, and (c) P(DVB-co-AN).

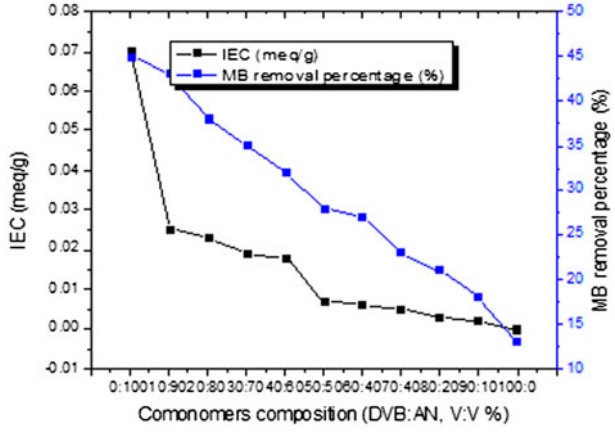


Fig. 10. Effect of monomers composition on IEC and MB removal percentage of HP(AN-co-DVB).

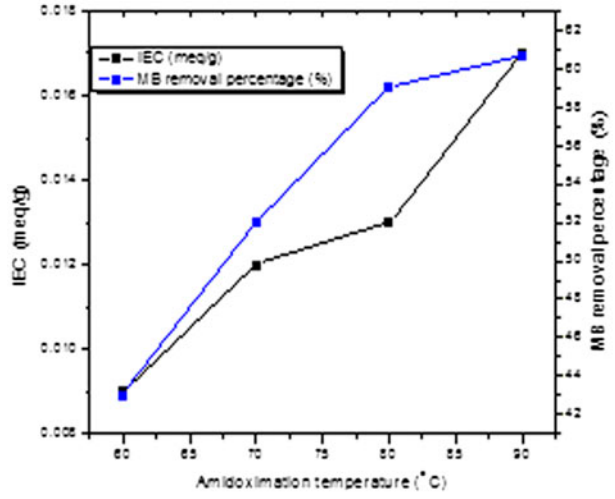


Fig. 11. Effect of amidoximation temperature on IEC and MB removal percentage of HP(AN-co-DVB).

### 3.3.3. Effect of the amidoximation time

The effect of variation of the amidoximation time with HA on the IEC of HP(AN-co-DVB) and its MB removal percentage was investigated as shown in Fig. 12. From the figure, it is clear that the IEC increased with increase in the amidooximation time till 5 h then it turned to be constant. This means that the reaction of this copolymer (AN-co-DVB, V:V, 50:50%) with hydroxylamine ended after 5 h reaction time under the studied amidoximation conditions, where the IEC increased from 0.002 to 0.010 (meq/g). On the other hand, the MB removal percentage was found to increase from 38 to 45% with increase in the reaction time from 1 to 6 h. The lower increment rate

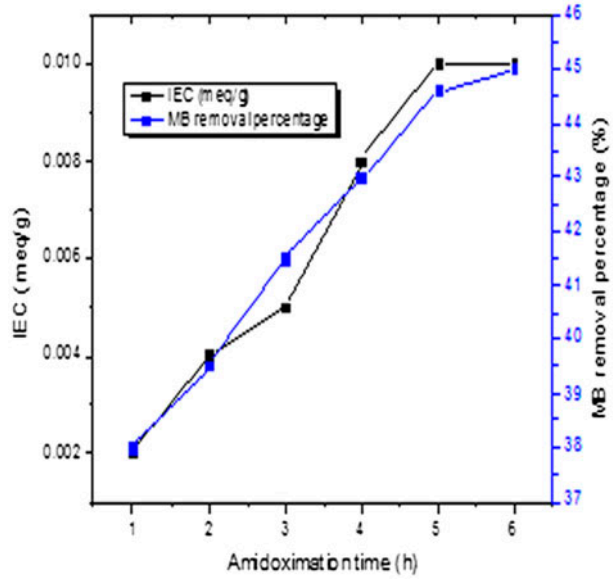


Fig. 12. Effect of amidoximation time on IEC and MB removal percentage of HP(DVB-co-AN).

of the MB removal percentage compared to the IEC increase may be referred to the adsorption of MB on the particles, surface as monolayer.

### 3.3.4. Effect of the HA concentration

Fig. 13 illustrates the effect of variation of the HA concentration on the IEC of HP(AN-co-DVB) and its MB removal percentage. From the figure, it is clear that the variation of the HA concentration from 0.5 to 3% increased the IEC almost linearly. The MB removal percentage was increased almost linearly from 30 to

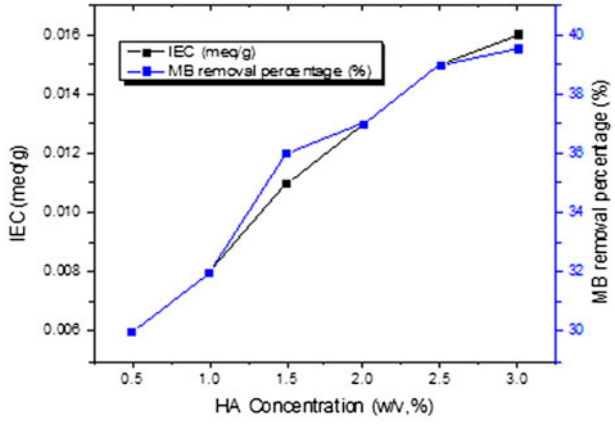


Fig. 13. Effect of HA concentration on IEC and MB removal percentage of HP(AN-co-DVB).

about 39.5%. The lower increment rate of the MB removal percentage compared to the IEC increase may be referred to the adsorption of MB on the particles surface as monolayer.

### 3.4. MB removal process

MB removal process using HP(DVB-co-AN) has been studied under different operational conditions. For comparison, P(DVB-co-AN) has been tested under the same operational conditions.

#### 3.4.1. Effect of the MB concentration

The effect of variation of the MB initial concentration on the copolymer's MB removal capacity is shown in Fig. 14. The MB removal percentages were decreased from 70 to 30% and from 66 to 26% of HP (DVB-co-AN) and P(DVB-co-AN), respectively. Such behavior can be attributed to the increase of the adsorbate amount to the unchanging number of available active sites on the adsorbent (since the amount of adsorbent is kept constant). The higher removal percentage of dye at low dye concentrations may be referred to interaction of all the MB molecules in the aqueous solution with the binding sites on the copolymer surface. However, at high dye concentrations, the dye adsorption percentages may be affected by the overload concentration, a situation affecting the adsorption distribution on the adsorbent surface sites. Also, the adsorption in case of HP(AN-co-DVB) is slightly higher than the adsorption in case of P (AN-co-DVB). Such behavior can be attributed to the presence of oximic groups.

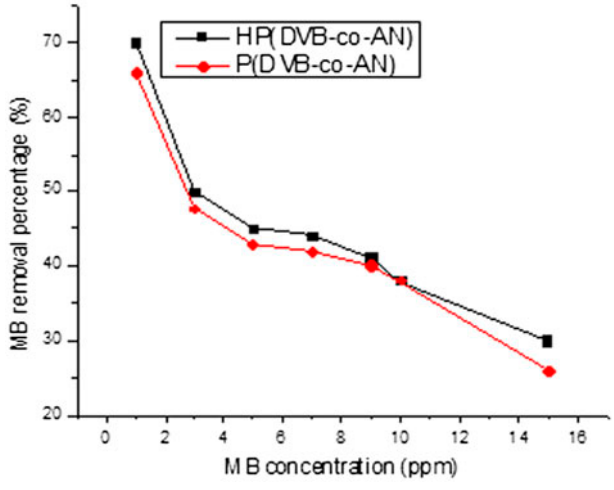


Fig. 14. Effect of initial dye concentration on MB removal percentage of HP(AN-co-DVB) and P(AN-co-DVB).

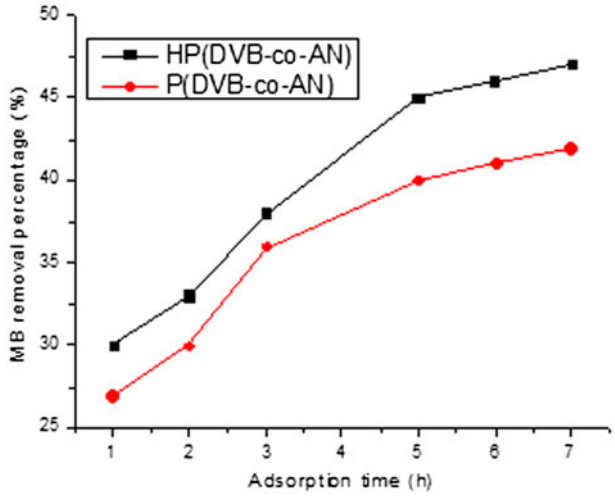


Fig. 15. Effect of contact time on MB removal percentage of HP(DVB-co-AN) and P(DVB-co-AN).

#### 3.4.2. Effect of the contact time

The effect of variation of the contact time on MB removal percentage was investigated (Fig. 15). From the figure, it can be seen that the MB removal percentage has been affected by increasing the contact time up to 5 h. Very slow equilibrium has been almost achieved after 7 h. Very fast surface adsorption process at the first 5 h, which consumed almost surface sites for adsorption, could give an explanation. Also, the adsorption in case of HP(AN-co-DVB) is slightly higher than the adsorption in case of P (AN-co-DVB).

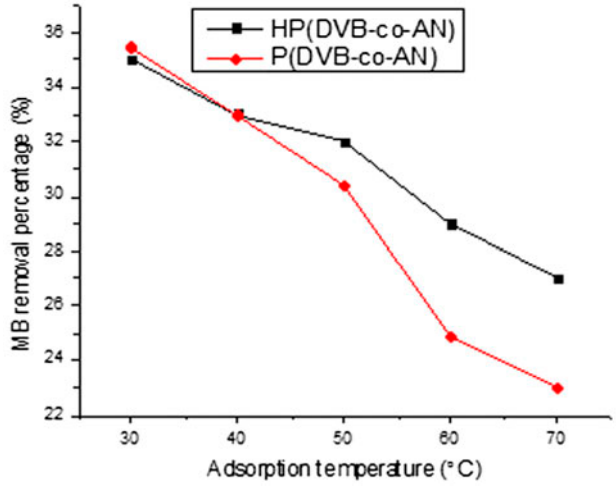


Fig. 16. Effect of adsorption temperature on MB removal percentage of HP(AN-co-DVB) and P(AN-co-DVB).

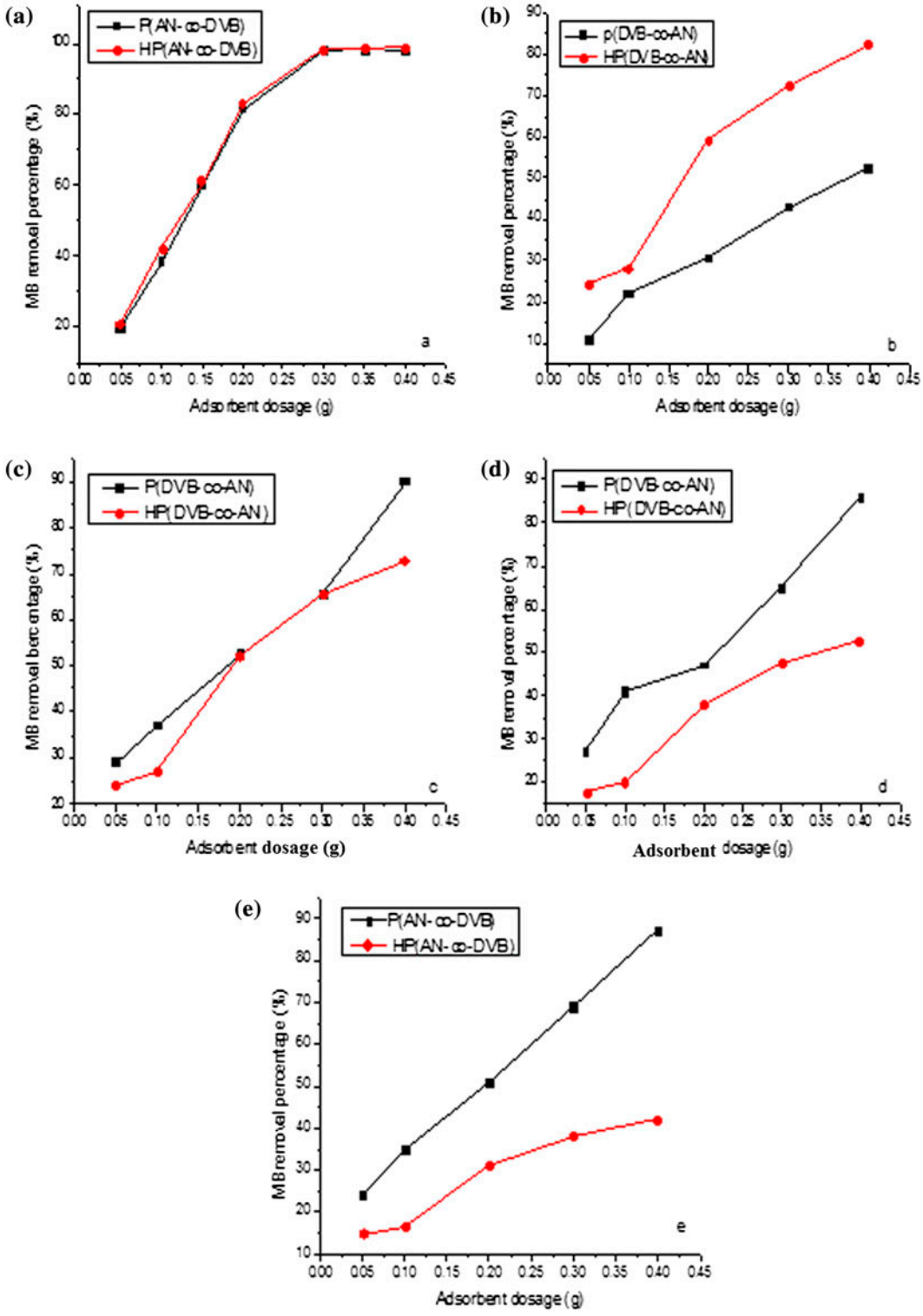


Fig. 17. Effect of adsorbent dosage on MB removal percentage of HP(AN-co-DVB) and P(AN-co-DVB), dye conc (a) 10 ppm, (b) 25 ppm, (c) 50 ppm, (d) 75 ppm, and (e) 100 ppm.

*3.4.3. Effect of the adsorption temperature*

Fig. 16 shows the effect of variation of the adsorption temperature over wide range, from 30 to 70˚C, on the MB removal percentage for both HP(AN-co-DVB) and P(AN-co-DVB). A decrease of removal percentage has been observed. The obtained results are considered an advantage, since the dye removal process does not need any additional heating and or other extra cost. This behavior may be referred to the acceleration effect of temperature on the dye molecules adsorption on the surface of both P(AN-co-DVB) and HP(AN-co-DVB) particles. This fast initial step reduces the concentration gradient between the MB dye liquid phase and the copolymer solid phase. MB concentration limitation from one side and high concentration of exchange sites over the particles surface in the other side contribute significantly to obtain this behavior. The absence of pore diffusion process also eliminates the effect of temperature [32].

*3.4.4. Effect of the adsorbent dosage*

The effect of variation of the adsorbent dosage on the MB percentage removal has been correlated at various MB concentrations (Fig. 17). It is evident from the curves that the dye percentage removal increases with adsorbent dosage. Such behavior is obvious because the number of active sites available for dye removal would be more as the amount of adsorbent increases. Also, HP(AN-co-DVB) shows advantages over P(AN-co-DVB) in the MB adsorption at dye concentration ranged from 10 to 25 ppm. Such behavior can be attributed to the oximic groups. However, P(AN-co-DVB) shows advantages over HP(AN-co-DVB) in adsorption of MB at concentration ranged from 75 to 100 ppm. Such behavior can be attributed to the fast adsorption initial step on the HP(AN-co-DVB) particles' surface, where creation of dye layer decreases the concentration gradient between the particles' solid surface and dye solution phase. Careful selection of the solid:liquid ratio is a crucial factor in the surface adsorption processes.

## 4. Conclusions

P(AN-co-DVB) nanoparticles (41 nm) has been prepared by precipitation polymerization technique. P (AN-co-DVB) has been functionalized with hydro oximic groups through reaction with hydroxyl amine hydrochloride. As a result, the particle size of the copolymer was increased from 41 up to 46 nm. Both copolymers, P(AN-co-DVB) and HP(AN-co-DVB), were tested in removal of MB from aqueous solution. Studies of the effect of some process variables including the contact time, the adsorbent dosage, the initial dye concentration, and the temperature on the adsorption process were carried out. HP(AN-co-DVB) shows advantages over P(AN-co-DVB) in adsorption of MB ranged from 10 to 25 ppm; however, P(AN-co-DVB) shows advantages over HP(AN-co-DVB) in adsorption of MB ranged from 75 to 100 ppm.

## References

[1] M.M. Abd El-Latif, A.M. Ibrahim, Adsorption, kinetic and equilibrium studies on removal of basic dye from aqueous solutions using hydrolyzed oak sawdust, Desalin. Water Treat. 6 (2009) 252–268.
[2] M. Leszczyńska, Z. Hubicki, Application of weakly and strongly basic anion exchangers for the removal of brilliant yellow from aqueous solutions, Desalin. Water Treat. 2 (2009) 156–161.
[3] A.E. Ofomaja, Equilibrium sorption of methylene blue using mansonia wood sawdust as biosorbent, Desalin. Water Treat. 3 (2009) 1–10.
[4] S. Rosenbaum, Dyeing of polyacrylonitrile fibers: I. Rates of diffusion with malachite green and diffusion model, J. Appl. Polym. Sci. 7 (1963) 1225–1242.
[5] S. Rosenbaum, Dyeing of polyacrylonitrile fibers: Part II: Experimental methods and dyeing rate with cationic and anionic dye, Text. Res. J. 34 (1964) 52–60.
[6] T.M.A. Hossain, H. Maeda, T. Iijima, Z. Morita, Diffusion of cationic dye into polyacrylonitrile, J. Polym. Sci., Part C: Polym. Lett. 5 (1967) 1069–1072.
[7] D. Şuteu, D. Bilba, C. Zaharia, HPAN textile fiber wastes for removal of dyes from industrial textile effluent, Bulletin of the Transilvania University of Braşov, Series I 2 (2009) 218–223.
[8] L. Boguslavsky, S. Baruch, S. Margel, Synthesis and characterization of polyacrylonitrile nanoparticles by dispersion/emulsion polymerization process, J. Colloid Interface Sci. 289 (2005) 71–85.
[9] T. Biswal, P.K. Sahoo, Synthesis of PAN nanoparticles via nonconventional microemulsion technique using Co (II)/ EDTA in suit complex, Ind. J. Chem. Technol. 14 (2007) 119–125.
[10] J.-M. Lee, S-J. Kang, S-J. Park, Synthesis of polyacrylonitrile based nanoparticles via aqueous dispersion polymerization, Macromol. Res. 17 (2009) 817–820.
[11] T. Biswal, R. Samal, P.K. Sahoo, Complex-mediated microwave- assisted synthesis of polyacrylonitrile nanoparticles, Nanotechnol. Sci. Appl. 3 (2010) 77–83.
[12] M. Rikukawa, D. Inagaki, K. Kaneko, Y. Takeoka, I. Ito, Y. Kanzaki, K. Sanui, Proton conductivity of smart membranes based on hydrocarbon polymers having phosphoric acid groups, J. Mol. Struct. 739 (2005) 153–161.
[13] A.R. Samarkandy, Synthesis of new polymeric composite materials and its application in sizing of cotton textiles, Appl. Sci. Res. 5 (2005) 330–340.
[14] C.M. Tseng, Y.Y. Lu, M.S. El-Aasser, J.W. Vanderhoff, Uniform polymer particles by dispersion polymerization in alcohol, J. Polym. Sci., Part A: Polym. Chem. 24 (1986) 2995–3007.

[15] E.D.S.S. Shen, M.S. Sudol, Control of particle size in dispersion polymerization of methyl methacrylate, J. Polym. Sci., Part A: Polym. Chem. 31 (1993) 1393–1402.
[16] A.J. Paine, W. Luymes, J. McNulty, Dispersion polymerization of styrene in polar solvents. 6. Influence of reaction parameters on particle size and molecular weight in poly(N-vinylpyrrolidone)-stabilized reactions, Macromolecules 23 (1990) 3104–3109.
[17] F. Candau, R.H. Ottewill, An Introduction to Polymer Colloids, Kluwer Academic, Dordrecht, 1990.
[18] P. Christian, M. R. Giles, R.M. T. Griffiths, D. J. Irvine, R. C. Major, S. M. Howdle, Free radical polymerization of methyl methacrylate in supercritical carbon dioxide using a pseudo-graft stabilizer: Effect of monomer, initiator, and stabilizer concentrations, Macromolecules 33 (2000) 9222–9227.
[19] Y. Chen, H.W. Yang, Hydroxypropyl cellulose (HPC) stabilized dispersion polymerization of styrene in polar solvents: Effect of reaction parameters, J. Polym. Sci., Part A: Polym. Chem. 30 (1992) 2765–2772.
[20] D.S. Yun, H. Lee, H.G. Jang, J.W. Yoo, Controlling size and distribution for nano-sized polystyrene spheres, Bull. Korean Chem. Soc. 31 (2010) 1345–1438.
[21] J.M. Sáenz, J.M. Asua, Kinetics of the dispersion copolymerization of styrene and butyl acrylate, Macromolecules 31 (1998) 5215–5222.
[22] D. Horák, Effect of reaction parameters on the particle size in the dispersion polymerization of 2-hydroxyethyl methacrylate, J. Polym. Sci., Part A: Polym. Chem. 37 (1999) 3785–3792.
[23] I. Capek, Emulsion polymerization of butyl acrylate, 2. Effect of the initiator type and concentration, Macromol. Chem. Phys. 195 (1994) 1137–1146.
[24] I. Capek, and L.Q. Tuan, Emulsion copolymerization of methyl methacrylate with ethyl acrylate, 1. Effect of the initiator concentration on the polymerization behaviour, Die Makromolek. Chem. 187 (1986) 2063–2072.
[25] I. Capek, Emulsion polymerization of butyl acrylate IV. Effects of initiator type and concentration, Polym. J. 26 (1994) 1154–1162.
[26] S. Sajjadi, B. Brooks, Butyl acrylate batch emulsion polymerization in the presence of sodium lauryl sulphate and potassium persulphate, J. Polym. Sci., Part A: Polym. Chem. 37 (1999) 3957–3972.
[27] H. Bamnolker, S. Margel, Dispersion polymerization of styrene in polar solvents: Effect of reaction parameters on microsphere surface composition and surface properties, size and size distribution, and molecular weight, J. Polym. Sci., Part A: Polym. Chem. 34 (1996) 1857–1871.
[28] F.L. Baines, N.C. Billiugham, S.P. Armes, Use of block copolymer stabilizers for the dispersion polymerization of styrene in alcoholic media, Macromolecules 29 (1996) 3096–3102.
[29] D. Horak, M. Karpisek, J. Turkova, M. Benes, Hydrazide-functionalized poly(2-hydroxyethyl methacrylate) microspheres for immobilization of horseradish peroxidase, Biotechnol. Progr. 15 (1999) 208–215.
[30] J.M.S. Asua, Kinetics of the dispersion copolymerization of styrene and butyl acrylate, Macromolecules 31 (1998) 5215–5222.
[31] S. Shen, E.D. Sudol, M.S. El-Aasser, Dispersion polymerization of methyl methacrylate: Mechanism of particle formation, J. Polym. Sci., Part A: Polym. Chem. 32 (1994) 1087–1100.
[32] M.S. Mohy Eldin, S.A. El-Sakka, M.M. El-Masry, I.I. Abdel-Gawad, S.S. Garybe, Removal of methylene blue dye from aqueous medium by nano poly acrylonitrile particles, Desalin. Water Treat. 44 (2012) 151–160.